Appl. Math. Mech. -Engl. Ed., **38**(10), 1459–1470 (2017)
DOI 10.1007/s10483-017-2242-6

Applied Mathematics and Mechanics (English Edition)

Thermal buckling and postbuckling of FGM circular plates with in-plane elastic restraints*

Yun SUN, Maolin WANG, Shirong LI†

School of Civil Science and Engineering, Yangzhou University,
Yangzhou 225127, Jiangsu Province, China

Abstract Based on von Karman's plate theory, the axisymmetric thermal buckling and post-buckling of the functionally graded material (FGM) circular plates with in-plane elastic restraints under transversely non-uniform temperature rise are studied. The properties of the FGM media are varied through the thickness based on a simple power law. The governing equations are numerically solved by a shooting method. The results of the critical buckling temperature, post-buckling equilibrium paths, and configurations for the in-plane elastically restrained plates are presented. The effects of the in-plane elastic restraints, material property gradient, and temperature variation on the responses of thermal buckling and post-buckling are examined in detail.

Key words functionally graded material (FGM) circular plate, in-plane elastic restraint, thermal post-buckling, shooting method, equilibrium path

Chinese Library Classification O343.1
2010 Mathematics Subject Classification 74K20, 74B05

1 Introduction

Functionally graded materials (FGMs) are known as a class of novel materials, in which the material properties vary smoothly and continuously in one, two, or even three specific directions. The advantage of these materials is that they can withstand high-temperature gradient environments while maintaining their structural integrities. The main application of FGMs is in high-temperature environments. Consequently, the thermal buckling and post-buckling analysis of FGM plates have attracted researchers' attention in recent years. Especially, circular/annular plates are known as a main branch of solid structures with wide applications in structural, mechanical, and civil engineering.

Some investigations have been carried out on the thermal buckling and post-buckling analyses of circular/annular FGM plates. Based on the classical plate theory (CPT), some works[1–9] on thermal circular/annular FGM plates have been performed. Najafizadeh and Eslami[1] investigated the thermal buckling analysis of circular FGM plates, and obtained the closed-form solutions for the buckling temperature. Ma and Wang[2] studied the thermal post-buckling of FGM circular plates by use of the shooting method. Li et al.[3] studied the nonlinear thermo-mechanical post-buckling of a circular FGM plate with geometric imperfection, and used the

* Received Oct. 12, 2016 / Revised Apr. 25, 2017
Project supported by the National Natural Science Foundation of China (Nos. 11272278 and 11672260) and the China Postdoctoral Science Foundation (No. 149558)
† Corresponding author, E-mail: srli@yzu.edu.cn

shooting method to solve the governing equations of the clamped plates. Kiani and Eslami[4] analyzed the linear and nonlinear stability behaviors of a thin FGM plate subjected to the uniform temperature and the constant angular velocity loadings. In the linear stability analysis, the critical buckling temperature was given by solving the stability equations via an exact closed-form solution and a power series method. Aghelinejad et al.[5] presented the nonlinear bending and axisymmetric thermal buckling and post-buckling analysis of a thin functionally graded (FG) annular plate, and solved the nonlinear ordinary differential equations with clamped-clamped boundary conditions numerically by the shooting method. Based on the finite element method, Ghomshei and Abbasi[6] investigated the axisymmetric thermal buckling of the FGM annular plates with variable thickness subjected to radially distributed thermal load. Kiani and Eslami studied the effect of the elastic foundation on the critical buckling temperature of FGM circular[7]/annular[8] plates. Sun and Li[9] studied the thermal post-buckling of an FGM circular plate with a rigid point constraint away from the center of the plate with a small interval by use of the shooting method.

The investigations on the thermal buckling and post-buckling of circular/annular FGM plates based on the first-order shear deformation plate theory (FSDT) can be referred to Refs. [10]–[15]. Najafizadeh and Hedayati[10] studied the axisymmetric thermal buckling of moderately thick circular FGM plates, and presented the closed-form solutions for the buckling temperature. Jalali et al.[11] carried out the thermal buckling of the sandwich plate with a homogenous variable thickness core and two constant thickness FGM face sheets. The stability equations were solved numerically by use of the pseudo-spectral method to evaluate the critical temperature rise. With the Mindlin formulation, Prakash and Ganapathi[12] analyzed the axisymmetric thermal buckling and vibration characteristics of FGM circular plates through the finite element approach. Kiani and Eslami[13] analyzed the thermal post-buckling of FGM circular plates with the consideration of the initial imperfection, temperature dependency, and through-the-thickness gradient, and obtained the equivalent properties of the FGM media based on three different homogenization schemes. Ghiasian et al.[14] presented an exact analytical approach to study the thermal buckling of the through-the-thickness annular FGM plate with temperature-dependent material properties, and obtained the equilibrium equations in the case of asymmetric deformation. They concluded that the fundamental buckling pattern of a symmetrically heated annular plate might be asymmetric in many cases. Based on the differential quadrature method, Sepahi et al.[15] investigated the thermal buckling and post-buckling of an FGM annular plate with the temperature-dependent material properties graded in the radial direction.

Very few analyses on the thermal buckling and post-buckling of FGM circular/annular plates based on the high order shear deformation plate theory (HSDT) have been found in the open literature. Najafizadeh and Heydari[16] studied the axisymmetric thermal buckling of the thick circular plates made of FGMs based on Reddy's plate theory, and presented the closed-form solution for the critical buckling temperature. Tran et al.[17] addressed an isogeometric finite element approach for the thermal buckling analysis of FGM plates, and provided the numerical results of circular and rectangular plates.

All of the above researches are developed on the assumptions that the plates have ideal or classical boundary conditions (clamped, simply supported, and free). However, in practical engineering, in some cases, the edge restraints should be considered as elastic supports. Wang and Wang[18], Laura et al.[19], Varma and Rao[20], and Rao and Rao[21–23] have considered the effects of elastic restraints in their studies for the transverse deformation of homogenous plates. Alipour[24] presented the static analysis of the FG sandwich circular plates with general elastic supported edge conditions. Bedroud et al.[25] studied the buckling analysis of the FG circular/annular nanoplates with concentric internal ring support and elastically restrained edges. In the above mentioned works[18–25], only Ref. [20] deals with the thermal post-buckling of circular plates with elastic restraints.

In the present paper, we will investigate the effect of the in-plane elastic restraints at the edge on the thermal buckling and post-buckling responses of FGM circular plates. Based on the geometrical nonlinear plate theory in von Karman's version, the axisymmetric thermal buckling and post-buckling responses of FGM circular plates with in-plane elastic restraints are studied by use of the shooting method. The effects of the in-plane elastic restraints, material gradient, and temperature variation on the critical thermal load, thermal post-buckling equilibrium path, and plate deformation will be analyzed.

2 Problem formulation

Consider the FGM circular plates with the radius a and the thickness h. A cylindrical coordinate system (r, θ, z) is defined with its origin located at the geometrical mid-plane of the plate, where r, θ, and z represent the coordinates in the radial, circumferential, and thickness directions, respectively. It is assumed that the plate edge is constrained elastically in the radial direction. The restraint forces are simplified as the radial resultant forces, which linearly distribute along the boundary. Therefore, the restraints can be simplified as linearly elastic translational springs with the stiffness $k_{\rm s}$, which are in the mid-plane of the plate and distribute continuously along the edge (see Fig. 1). If $k_{\rm s} \to \infty$, the edge supports in Mode I and Mode II are simplified as the immovable clamped and simply supported edges, respectively.

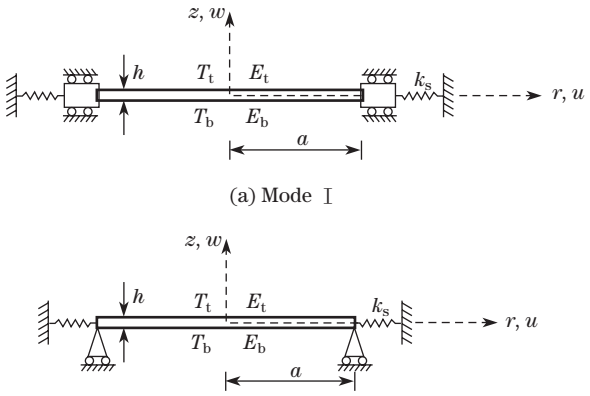

Fig. 1 Geometry, edge supports, and coordinates of the FGM circular plates

2.1 Gradients of material properties

The plate is assumed to be composed of two constituents, whose volume fractions change continuously and smoothly in the thickness direction. According to the linear rule of mixture, the effective material properties of FGMs, such as Young's modulus E, Poisson's ratio μ, thermal conductivity κ, and thermal expansion coefficient α, can be expressed uniformly as follows:

$$P(z) = P_{\rm b}V_{\rm b} + P_{\rm t}V_{\rm t} = P_{\rm b}\psi_{\rm P}(z), \quad P = E, \mu, \kappa, \alpha, \tag{1}$$

in which $\psi_{\rm P}(z)$ is given based on the simple power law

$$\psi_{\rm P}(z) = 1 + (P_{\rm r} - 1)(0.5 + z/h)^n, \quad P = E, \mu, \kappa, \alpha, \tag{2}$$

where the superscript n is the volume fraction exponent, $n \in [0, \infty)$, $P_{\rm t}$ and $P_{\rm b}$ are the properties of pure materials at the top and bottom surfaces, respectively, and $P_{\rm r} = P_{\rm t}/P_{\rm b}$. Usually, Poisson's ratio of the FGMs changes very little so that it is assumed to be a constant in this paper for the analysis convenience.

2.2 Temperature profile

The temperature rise is assumed to vary only along the thickness direction. The non-uniform temperature rise field is obtained by solving the one-dimensional steady-state heat conduction equation with the specified boundary conditions as follows[26]:

$$T(z) = T_{\mathrm{b}} t(z), \tag{3}$$

where

$$t(z) = 1 + (T_{\mathrm{r}} - 1) \int_{-h/2}^{z} \frac{\mathrm{d}z}{\psi_\kappa(z)} \Big(\int_{-h/2}^{h/2} \frac{\mathrm{d}z}{\psi_\kappa(z)} \Big)^{-1}. \tag{4}$$

In the above equations, $T_{\mathrm{r}} = T_{\mathrm{t}}/T_{\mathrm{b}}$, where $T_{\mathrm{t}} = T(h/2)$ and $T_{\mathrm{b}} = T(-h/2)$ are the temperature rise at the top and bottom surfaces of the plate, respectively. For the convenience of the following analysis, it is further assumed that $T_{\mathrm{b}} \neq 0$. If $T_{\mathrm{r}} = 1$, the temperature rise is uniform.

2.3 Governing equations

According to von Karman's plate theory, the dimensionless governing equations for the axisymmetric thermal post-buckling of the circular plate are[9]

$$\frac{\mathrm{d}^2 U}{\mathrm{d}x^2} + \frac{1}{x}\frac{\mathrm{d}U}{\mathrm{d}x} - \frac{U}{x^2} + \frac{\mathrm{d}W}{\mathrm{d}x}\frac{\mathrm{d}^2 W}{\mathrm{d}x^2} + \frac{1-\mu}{2x}\Big(\frac{\mathrm{d}W}{\mathrm{d}x}\Big)^2 - \frac{\phi_2}{\phi_1}\frac{1}{\beta}\Big(\frac{\mathrm{d}^3 W}{\mathrm{d}x^3} + \frac{1}{x}\frac{\mathrm{d}^2 W}{\mathrm{d}x^2} - \frac{1}{x^2}\frac{\mathrm{d}W}{\mathrm{d}x}\Big) = 0, \tag{5}$$

$$\begin{aligned} &-\Big(\frac{\mathrm{d}^4 W}{\mathrm{d}x^4} + \frac{2}{x}\frac{\mathrm{d}^3 W}{\mathrm{d}x^3} - \frac{1}{x^2}\frac{\mathrm{d}^2 W}{\mathrm{d}x^2} + \frac{1}{x^3}\frac{\mathrm{d}W}{\mathrm{d}x}\Big) + 12\beta^2 c\phi_1 \Big(\Big(\frac{\mathrm{d}U}{\mathrm{d}x} + \frac{1}{2}\Big(\frac{\mathrm{d}W}{\mathrm{d}x}\Big)^2 + \mu\frac{U}{x}\Big)\frac{\mathrm{d}^2 W}{\mathrm{d}x^2} \\ &+ \Big(\mu\frac{\mathrm{d}U}{\mathrm{d}x} + \frac{\mu}{2}\Big(\frac{\mathrm{d}W}{\mathrm{d}x}\Big)^2 + \frac{U}{x}\Big)\frac{1}{x}\frac{\mathrm{d}W}{\mathrm{d}x}\Big) - 12\beta c\phi_2\Big(\Big(\frac{\mathrm{d}^2 W}{\mathrm{d}x^2} + \mu\frac{1}{x}\frac{\mathrm{d}W}{\mathrm{d}x}\Big)\frac{\mathrm{d}^2 W}{\mathrm{d}x^2} \\ &+ \Big(\mu\frac{\mathrm{d}^2 W}{\mathrm{d}x^2} + \frac{1}{x}\frac{\mathrm{d}W}{\mathrm{d}x}\Big)\frac{1}{x}\frac{\mathrm{d}W}{\mathrm{d}x}\Big) - c\phi_4\tau\Big(\frac{\mathrm{d}^2 W}{\mathrm{d}x^2} + \frac{1}{x}\frac{\mathrm{d}W}{\mathrm{d}x}\Big) = 0. \end{aligned} \tag{6}$$

The continuous conditions at the center $x = \eta$ are

$$U = 0, \quad \frac{\mathrm{d}W}{\mathrm{d}x} = 0, \quad \frac{\mathrm{d}^3 W}{\mathrm{d}x^3} + \frac{1}{x}\frac{\mathrm{d}^2 W}{\mathrm{d}x^2} = 0, \tag{7}$$

where η is a small number introduced to avoid the singularity at the center $x = 0$ in the following numerical computation.

The boundary conditions at $x = 1$ are given as follows:

(i) Mode I

$$12\phi_1\beta^2\Big(\frac{\mathrm{d}U}{\mathrm{d}x} + \mu U\Big) - 12\phi_2\beta\frac{\mathrm{d}^2 W}{\mathrm{d}x^2} - \phi_4\tau + K_s U = 0, \quad W = 0, \quad \frac{\mathrm{d}W}{\mathrm{d}x} = 0. \tag{8}$$

(ii) Mode II

$$\begin{cases} 12\phi_1\beta^2\Big(\dfrac{\mathrm{d}U}{\mathrm{d}x} + \dfrac{1}{2}\Big(\dfrac{\mathrm{d}W}{\mathrm{d}x}\Big)^2 + \mu U\Big) - 12\phi_2\beta\Big(\dfrac{\mathrm{d}^2 W}{\mathrm{d}x^2} + \mu\dfrac{\mathrm{d}W}{\mathrm{d}x}\Big) - \phi_4\tau + K_s U = 0, \\ W = 0, \\ 12\beta^2\phi_2\Big(\dfrac{\mathrm{d}U}{\mathrm{d}x} + \dfrac{1}{2}\Big(\dfrac{\mathrm{d}W}{\mathrm{d}x}\Big)^2 + \mu U\Big) - \beta\phi_3\Big(\dfrac{\mathrm{d}^2 W}{\mathrm{d}x^2} + \mu\dfrac{\mathrm{d}W}{\mathrm{d}x}\Big) - \phi_5\tau = 0. \end{cases} \tag{9}$$

In the governing equations (5) and (6) and the boundary conditions (7)–(9), the dimensionless variables are defined by

$$\begin{cases} (x, U, W) = \dfrac{1}{a}(r, u, w), \quad \beta = \dfrac{a}{h}, \quad \tau = 12(1+\mu)\beta^2\alpha_{\rm b}T_{\rm b}, \\ K_{\rm S} = \dfrac{k_s a^3}{D_b}, \quad c = \dfrac{1}{\phi_3 - 12\phi_2^2/\phi_1}, \end{cases} \tag{10}$$

where U and W are the displacements in the mid-plane of the plate along the r- and z-directions, respectively. β is the ratio of radius to thickness. τ is the dimensionless temperature rise for the homogenous plate made of pure material at the bottom surface subjected to the uniform temperature rise at the bottom surface, which is defined as the referenced thermal load. $K_{\rm S}$ is the dimensionless in-plane spring stiffness. $D_{\rm b} = E_{\rm b}h^3/(12(1-\mu^2))$ is the bending rigidity of the homogenous plate made of pure material at the bottom surface. ϕ_i $(i = 1, 2, 3, 4, 5)$ are dimensionless parameters depending on the material gradient and temperature variation in the thickness direction[9], and they are defined by

$$\begin{cases} \phi_1 = \dfrac{1}{h}\displaystyle\int_{-h/2}^{h/2} \psi_E(z){\rm d}z, \quad \phi_2 = \dfrac{1}{h^2}\int_{-h/2}^{h/2} \psi_E(z)z{\rm d}z, \quad \phi_3 = \dfrac{12}{h^3}\int_{-h/2}^{h/2} \psi_E(z)z^2{\rm d}z, \\ \phi_4 = \dfrac{1}{h}\displaystyle\int_{-h/2}^{h/2} \psi_E(z)\psi_\alpha(z)t(z){\rm d}z, \quad \phi_5 = \dfrac{1}{h^2}\int_{-h/2}^{h/2} \psi_E(z)\psi_\alpha(z)t(z)z{\rm d}z. \end{cases} \tag{11}$$

If the plate is homogeneous, $\phi_2 = 0$. If the plate is subjected to the uniform temperature rise, $\phi_5 = 0$. For the metal-rich plate, $c = 1$.

3 Numerical results and discussion

The governing equations (5) and (6) associated with the boundary conditions (7)–(9) constitute the two-point boundary value problem of nonlinear ordinary differential equations. It is difficult to get the analytical solution. The shooting method[27–29] is used to solve the problem numerically. The two-point boundary value problem is replaced by a sequence of initial-value problems. The unknown values of the equations at the initial point are estimated to start the computation. They are iterated upon with modified values until the prescribed boundary conditions at the final point are satisfied.

In the following numerical computation, the plate is assumed to be composed of ceramic and metal. The ceramic constituent is zirconia (ZrO_2), and the metal constituent is aluminum (Al). The material constants of the two constituents are given as follows[30]:

$$\begin{aligned} {\rm ZrO_2}\text{:}\ & E_{\rm t} = E_{\rm c} = 151\,{\rm GPa}, \quad \alpha_{\rm t} = \alpha_{\rm c} = 10\times10^{-6}{\rm K}^{-1}, \\ & \kappa_{\rm t} = \kappa_{\rm c} = 2.09\,{\rm W/(m\cdot K)}, \quad \mu_{\rm t} = \mu_{\rm c} = 0.3; \\ {\rm Al}\text{:}\ & E_{\rm b} = E_{\rm m} = 70\,{\rm GPa}, \ \alpha_{\rm b} = \alpha_{\rm m} = 23\times10^{-6}\,{\rm K}^{-1}, \\ & \kappa_{\rm b} = \kappa_{\rm m} = 204\,{\rm W/(m\cdot K)}, \ \mu_{\rm b} = \mu_{\rm m} = 0.3, \end{aligned}$$

where Poisson's ratio is assumed to be a constant, and the small number η is set to be 0.001. Expect for special explanation, the ratio of radius to thickness is selected to be $\beta = 30$ in the following numerical computation.

To assure the validity and accuracy of the present numerical method, a comparison study is conducted. When $K_{\rm S} \to \infty$, it is approximately $K_{\rm S} = 10^{13}$ herein, the edge support in Mode I may be modelled as an ideal immovable clamped edge. The dimensional critical buckling temperature rise defined as $\Delta T_{\rm cr} = \tau/(12(1+\mu)\alpha_{\rm m}\beta^2)$ for the FGM plates with immovable

clamped edge support under the uniform temperature rise is compared with that in the closed-form solutions of Najafizadeh and Hedayati[10] (see Table 1). For the comparison convenience, the material constants of the two constituents are $E_{\rm m} = 70\,{\rm GPa}$, $\alpha_{\rm m} = 23 \times 10^{-6}\,{\rm K}^{-1}$, $\kappa_{\rm m} = 204\,{\rm W/(m \cdot K)}$ for the metal constituent of aluminum and $E_{\rm c} = 380\,{\rm GPa}$, $\alpha_{\rm c} = 7.4 \times 10^{-6}\,{\rm K}^{-1}$, $\kappa_{\rm c} = 10.4\,{\rm W/(m \cdot K)}$ for the ceramic constituent of alumina. It is seen that good agreement is observed among the results, which shows the fine accuracy of the present numerical method.

Table 1 Dimensional critical buckling temperature differences $\Delta T_{\rm cr}$ (K) for the FGM plates with ideal immovable clamped edge support under uniform temperature rise ($T_{\rm r} = 1$)

β	n					
	0.0		0.5		1.0	
	Present	Ref. [10]	Present	Ref. [10]	Present	Ref. [10]
100	12.718	12.716	7.205	7.204	5.908	5.907
50	50.873	50.866	28.823	28.819	23.634	23.630
25	203.493	203.465	115.293	115.273	94.537	94.520
20	317.958	317.914	180.146	180.121	147.714	147.694

The dimensionless critical buckling temperature $\tau_{\rm cr}$ of the FGM plates with edge support in Mode I versus the spring stiffness parameter $K_{\rm S}$ for different values of the volume fraction exponent n and the temperature ratio $T_{\rm r}$ is depicted in Fig. 2. It can be seen that, when the spring stiffness increases, the critical buckling temperature decreases. This is because that, the thermal buckling is caused by the in-plane compressive membrane forces generated by the restriction to the thermal expansion. In other words, for a definite critical buckling load, which is equal to the external in-plane compressive force at the plate edge, a smaller value of the spring stiffness corresponds to a larger amount of the temperature rise. When the spring stiffness tends to be infinite, the critical buckling temperature tends to be the value of the plate with immovable clamped edge support. If the spring stiffness is too small, the circular plate cannot buckle because that the in-plane compressive forces produced by the elastic restraints are too small to bring forth the thermal buckling. For a given value of the spring stiffness, the critical buckling temperature of an FGM plate is intermediate between the two associated metal-rich and ceramic-rich homogenous plates. The critical buckling temperature rise with the decrease in the volume fraction exponent n. It can be explained that when n decreases, the ceramic constituent increases, which makes the bending rigidity of the plate larger.

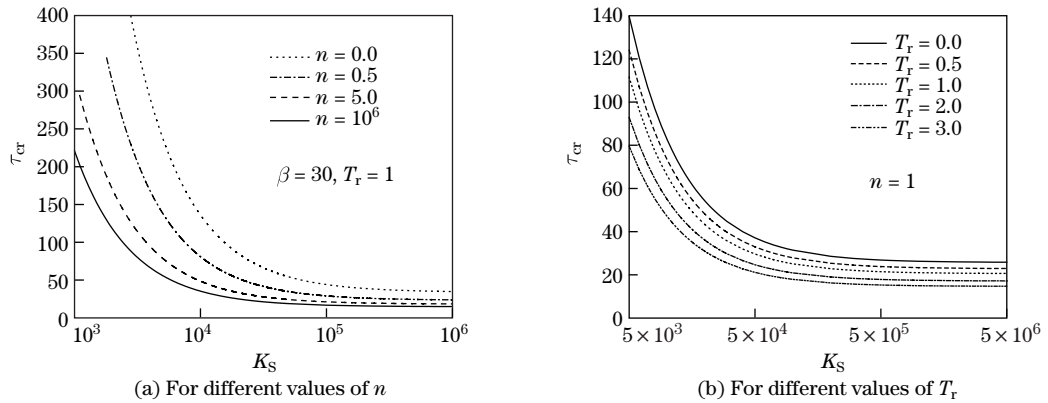

(a) For different values of n (b) For different values of $T_{\rm r}$

Fig. 2 Dimensionless critical buckling temperature $\tau_{\rm cr}$ versus the elastic stiffness $K_{\rm S}$ for the FGM plates with edge support in Mode I

Figure 3 shows the effect of the spring stiffness on the dimensionless critical buckling temperature for the circular plates with edge support in Mode II. When $K_S \to \infty$, the edge support in Mode II is modelled as the immovable simply supported edge. In this case, only the homogeneous plates under the uniform temperature rise have critical buckling temperatures. The critical buckling temperature of the metal-rich plate ($n = 10^6$) is lower than that of the ceramic-rich plate ($n = 0$). When the ratio of radius to thickness β increases, the critical buckling temperature rise. It can be explained that this ratio is included in the defined equation of the dimensionless temperature rise τ (see Eq. (10)).

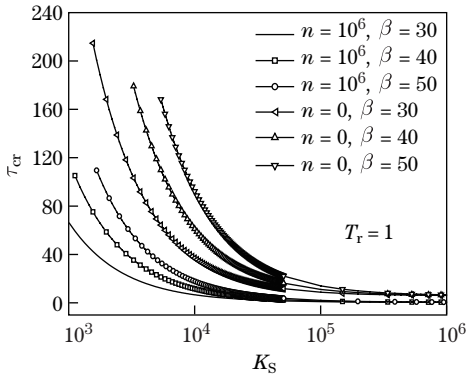

Fig. 3 Dimensionless critical buckling temperature τ_{cr} versus the spring stiffness K_S for the homogenous plates with edge support in Mode II under uniform temperature rise

Figure 4 gives the dimensionless critical radial displacement at the edge $U(1)_{cr}$ versus the spring stiffness K_S for different values of n. The critical radial displacement exists only in the homogeneous plates with the edge support of Mode II under the uniform temperature rise. The critical radial displacement decreases with the increase in the spring stiffness K_S. For a given value of K_S, when the volume fraction exponent n increases, the critical radial displacement decreases. From Fig. 4(b), it can be concluded that, for a given value of n, the critical radial displacement is irrelevant to β.

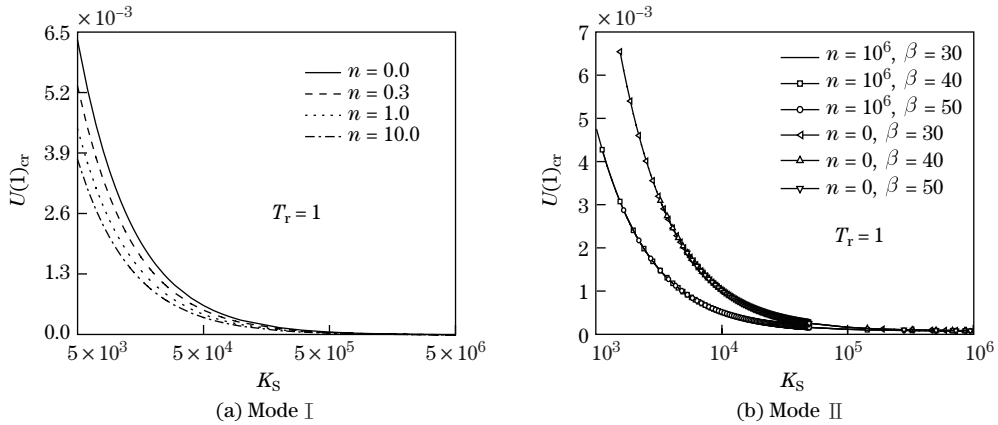

Fig. 4 Dimensionless critical radial displacement $U(1)_{cr}$ at the edge versus the spring stiffness K_S

The equilibrium paths of the thermal post-buckling deformation in terms of dimensionless central deflection $W(0)$ versus the spring stiffness K_S for the FGM plates with edge support in Mode II are plotted in Fig. 5. The central deflection increases with the increase in the

spring stiffness. The homogeneous plates ($n = 0, 10^6$) subjected to the uniform temperature rise can buckle along two directions, i.e., upward and downward. The inhomogeneous plates ($n = 0.2, 1.0$) under the uniform temperature rise and the FGM plates can only deflect along one direction, i.e., downward.

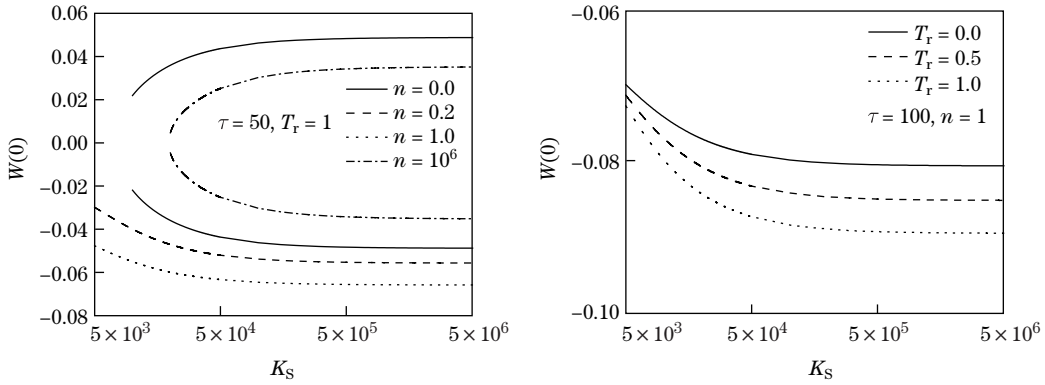

(a) For different values of n (b) For different values of T_r

Fig. 5 Dimensionless central deflection $W(0)$ versus the spring stiffness K_S for the FGM plates with edge support in Mode II

Figures 6 and 7 show the thermal post-buckling equilibrium paths in terms of the dimensionless central deflection $W(0)$ versus the temperature rise τ for the FGM circular plate. The variation of the central deflection with respect to the spring stiffness is monotonic. The higher the spring stiffness is, the larger the central deflection is. Apparently, the responses of the plates with edge support in Mode I are all the bifurcation-type buckling for all values of K_S and β. This is because that Eqs. (5) and (6) and the boundary conditions in Eq. (8) for the plate in Mode I consist of a standard eigenvalue problem, which is homogenous. However, for the plates with edge support in Mode II, only the buckling of homogenous plates under the uniform temperature rise is of the bifurcation type. The buckling of homogenous plates under the non-uniform temperature rise and the FGM plate are non-bifurcation form. Due to the existence of the thermal bending moment in the boundary conditions in Eq. (9), which is generated by the non-symmetric distribution of material properties and the temperature rise, Eqs. (5) and (6) and the boundary conditions (9) cannot be

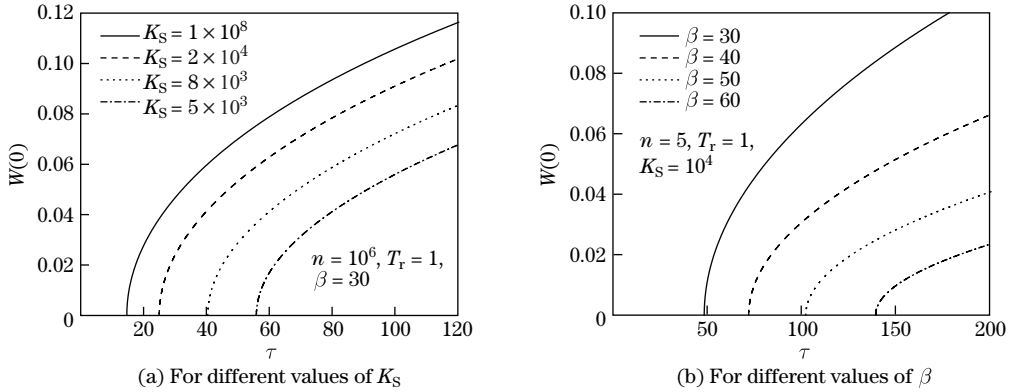

(a) For different values of K_S (b) For different values of β

Fig. 6 Dimensionless central deflection $W(0)$ versus the temperature rise τ for the FGM plates with edge support in Mode I

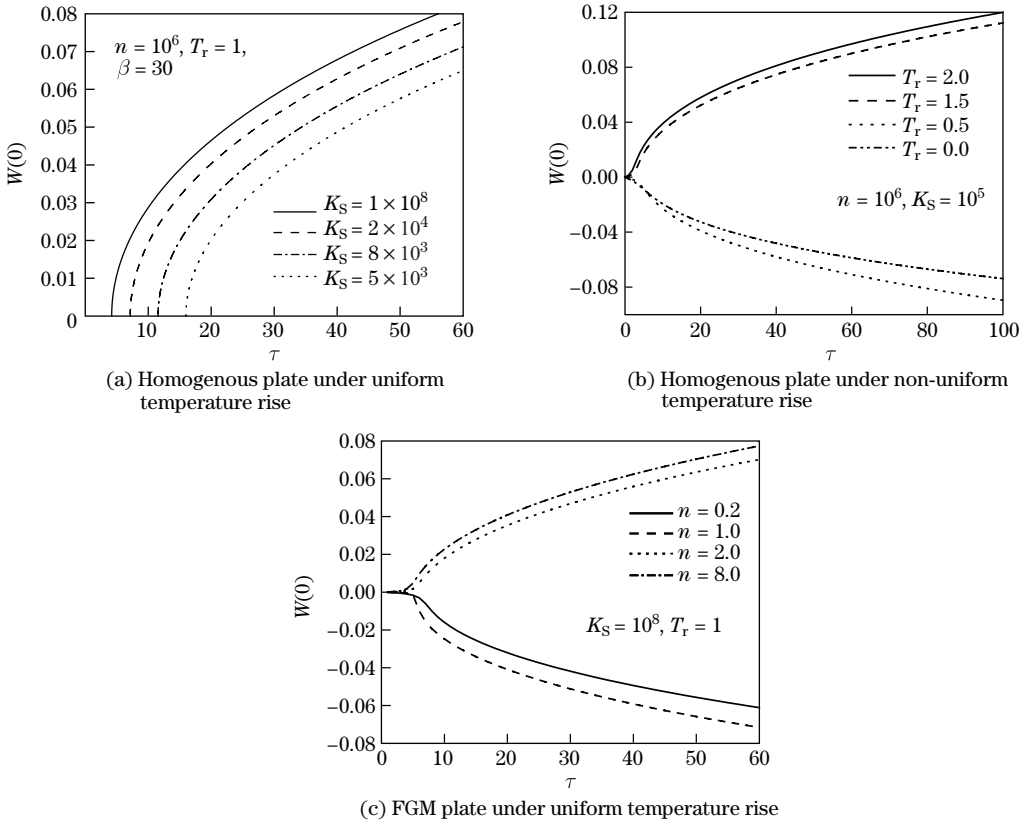

(a) Homogenous plate under uniform temperature rise

(b) Homogenous plate under non-uniform temperature rise

(c) FGM plate under uniform temperature rise

Fig. 7 Dimensionless central deflection $W(0)$ versus the temperature rise τ for the plates with edge support in Mode II

transformed into a standard eigenvalue problem, which is non-homogenous. The plates deflect at the heating onset. From Fig. 7(b), we can see that the homogenous plate deflects upward under the non-uniform temperature rise $T_{\mathrm{r}} = 1.5, 2$ and downward under $T_{\mathrm{r}} = 0, 0.5$. If $T_{\mathrm{r}} = 1.5, 2$, the temperature rise at the top surface is larger than that at the bottom surface. Therefore, the top surface expands greater than the bottom surface, the plate deflects upward. For the constituents of this study, under the uniform temperature rise, the FGM plates deflect upward for $n = 2, 8$ and downward for $n = 0.2, 1$ (see Fig. 7(c)).

The thermal post-buckling configurations for the FGM circular plates are plotted in Figs. 8 and 9. It is seen from these figures that, the lateral deflection increases with the increases in K_{S} and τ. We also can find that with the increases in n and T_{r}, the lateral deflection becomes larger.

4 Conclusions

Based on the geometrical nonlinear plate theory in von Karman's version, the axisymmetric thermal buckling and post-buckling responses of the FGM circular plate which is restricted by the in-plane elastic restraints of the translational springs are studied numerically by use of the shooting method. The temperature rise is considered to vary only along the thickness direction according to the one-dimensional steady-state heat conduction equation. The effective material properties are assumed to be varied as power law functions in the thickness direction. The effects of the in-plane spring stiffness parameter, the gradient of the material properties, the temperature variation, and the ratio of radius to width on the critical buckling temperature,

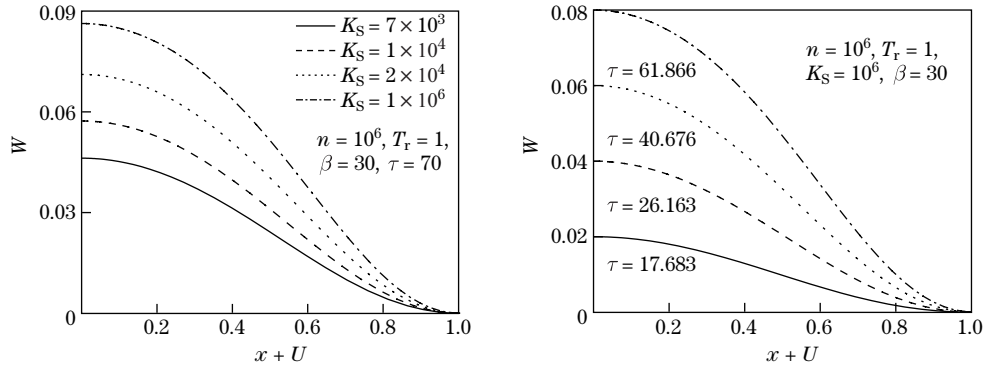

(a) For different values of K_S (b) For different values of τ

Fig. 8 Thermal post-buckling configurations for the plate with edge support in Mode I

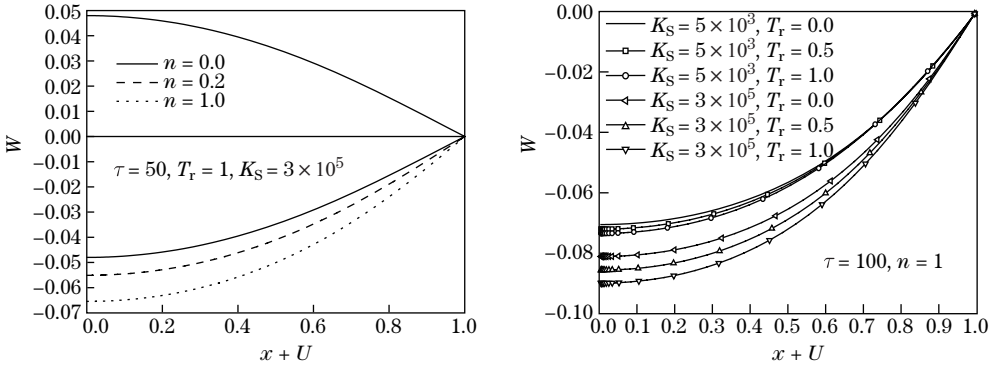

(a) For different values of n (b) For different values of T_r

Fig. 9 Thermal post-buckling configurations for the FGM plate with edge support in Mode II

the post-buckling equilibrium paths, and the configurations are examined. Some conclusions are drawn as follows:

(i) The critical buckling temperature decreases with the increase in the spring stiffness and volume fraction exponent. A lower temperature rise is needed for a plate with larger spring stiffness to buckle. When the volume fraction exponent increases, the metallic constituent increases, which makes the bending rigidity of the plate lower or the plate buckle easier.

(ii) When the spring stiffness increases, the radial displacement decreases, while the lateral deflection increases.

(iii) The responses of FGM circular plates with edge support in Mode I are all of the bifurcation type of buckling because both the governing equations and the boundary conditions in the transverse direction are homogenous. Therefore, the plate remains the undeflected state when $\tau < \tau_{cr}$, and buckles when $\tau \geqslant \tau_{cr}$.

(iv) For the plate with edge support in Mode II, only the buckling of the homogeneous plate under the uniform temperature rise is of the bifurcation type. The homogenous plate under the non-uniform temperature rise and the FGM plate all deflect at the heating onset, and reveal a unique and stable equilibrium path.

References

[1] Najafizadeh, M. M. and Eslami, M. R. First-order-theory-based thermoelastic stability of functionally graded material circular plates. *AIAA Journal*, **40**, 1444–1450 (2002)

[2] Ma, L. S. and Wang, T. J. Nonlinear bending and post-buckling of a functionally graded circular plate under mechanical and thermal loadings. *International Journal of Solids and Structures*, **40**, 3311–3330 (2003)

[3] Li, S. R., Zhang, J. H., and Zhao, Y. G. Nonlinear thermomechanical post-buckling of circular FGM plate with geometric imperfection. *Thin-Walled Structures*, **45**, 528–536 (2007)

[4] Kiani, Y. and Eslami, M. R. Nonlinear thermo-inertial stability of thin circular FGM plates. *Journal of the Franklin Institute*, **351**, 1057–1073 (2014)

[5] Aghelinejad, M., Zare, K., Ebrahimi, F., and Rastgoo, A. Nonlinear thermomechanical post-buckling analysis of thin functionally graded annular plates based on von-Karman's plate theory. *Mechanics of Advanced Materials & Structures*, **18**, 319–326 (2011)

[6] Ghomshei, M. M. and Abbasi, V. Thermal buckling analysis of annular FGM plate having variable thickness under thermal load of arbitrary distribution by finite element method. *Journal of Mechanical Science and Technology*, **27**, 1031–1039 (2013)

[7] Kiani, Y. and Eslami, M. R. Instability of heated circular FGM plates on a partial Winkler-type foundation. *Acta Mechanica*, **224**, 1045–1060 (2013)

[8] Kiani, Y. and Eslami, M. R. An exact solution for thermal buckling of annular FGM plates on an elastic medium. *Composites Part B*: *Engineering*, **45**, 101–110 (2013)

[9] Sun, Y. and Li, S. R. Thermal post-buckling of functionally graded material circular plates subjected to transverse point-space constraints. *Journal of Thermal Stresses*, **37**, 1153–1172 (2014)

[10] Najafizadeh, M. M. and Hedayati, B. Refined theory for thermoelastic stability of functionally graded circular plates. *Journal of Thermal Stresses*, **27**, 857–880 (2004)

[11] Jalali, S. K., Naei, M. H., and Poorsolhjouy, A. Thermal stability analysis of circular functionally graded sandwich plates of variable thickness using pseudo-spectral method. *Materials and Design*, **31**, 4755–4763 (2010)

[12] Prakash, T. and Ganapathi, M. Asymmetric flexural vibration and thermoelastic stability of FGM circular plates using finite element method. *Composites Part B*: *Engineering*, **37**, 642–649 (2006)

[13] Kiani, Y. and Eslami, M. R. Thermal postbuckling of imperfect circular functionally graded material plates: examination of voigt, Mori-Tanaka, and self-consistent schemes. *Journal of Pressure Vessel Technology*, **137**, 021201 (2015)

[14] Ghiasian, S. E., Kiani, Y., Sadighi, M., and Eslami, M. R. Thermal buckling of shear deformable temperature dependent circular/annular FGM plates. *International Journal of Mechanical Sciences*, **81**, 137–148 (2014)

[15] Sepahi, O., Forouzan, M. R., and Malekzadeh, P. Thermal buckling and postbuckling analysis of functionally graded annular plates with temperature-dependent material properties. *Materials and Design*, **32**, 4030–4041 (2011)

[16] Najafizadeh, M. M. and Heydari, H. R. Thermal buckling of functionally graded circular plates based on higher order shear deformation plate theory. *European Journal of Mechanics-A/Solids*, **23**, 1085–1100 (2004)

[17] Tran, L. V., Thai, C. H., and Nguyen-Xuan, H. An isogeometric finite element formulation for thermal buckling analysis of functionally graded plates. *Finite Elements in Analysis and Design*, **73**, 65–76 (2013)

[18] Wang, C. Y. and Wang, C. M. Buckling of circular plates with an internal ring support and elastically restrained edges. *Thin-Walled Structures*, **39**, 821–825 (2001)

[19] Laura, P. A. A., Gutiérrez, R. H., Sanzi, H. C., and Elvira, G. Buckling of circular, solid and annular plates with an intermediate circular support. *Ocean Engineering*, **27**, 749–755 (2000)

[20] Varma, R. R. and Rao, G. V. Novel formulation to study thermal postbuckling of circular plates with edges elastically restrained against rotation. *Journal of Engineering Mechanics*, **137**, 708–711 (2011)

[21] Rao, L. B. and Rao, C. K. Buckling analysis of circular plates with elastically restrained edges and resting on internal elastic ring support. *Mechanics Based Design of Structures and Machines*, **38**, 440–452 (2010)

[22] Rao, L. B. and Rao, C. K. Buckling of annular plates with elastically restrained external and internal edges. *Mechanics Based Design of Structures and Machines*, **41**, 222–235 (2013)

[23] Rao, L. B. and Rao, C. K. Buckling of circular plate with foundation and elastic edge. *International Journal of Mechanics & Materials in Design*, **11**, 149–156 (2014)

[24] Alipour, M. M. A novel economical analytical method for bending and stress analysis of functionally graded sandwich circular plates with general elastic edge conditions, subjected to various loads. *Composites Part B*: *Engineering*, **95**, 48–63 (2016)

[25] Bedroud, M., Nazemnezhad, R., Hosseini-Hashemi, S., and Valixani, M. Buckling of FG circular/annular Mindlin nanoplates with an internal ring support via nonlocal elasticity. *Applied Mathematical Modelling*, **40**, 3185–3210 (2015)

[26] Sun, Y., Li, S. R., and Batra, R. C. Thermal buckling and post-buckling of FGM Timoshenko beams on nonlinear elastic foundation. *Journal of Thermal Stresses*, **39**, 11–26 (2016)

[27] Li, S. R. and Zhou, Y. H. Nonlinear vibration of heated orthotropic annular plates with immovably hinged edges. *Journal of Thermal Stresses*, **26**, 691–700 (2003)

[28] Li, S. R., Su, H. D., and Cheng, C. J. Free vibration of functionally graded material beams with surface-bonded piezoelectric layers in thermal environment. *Applied Mathematics and Mechanics* (*English Edition*), **30**(9), 969–982 (2009) DOI 10.1007/s10483-009-0803-7

[29] Li, S. R. and Batra, R. C. Thermal buckling and post-buckling of Euler-Bernoulli beams supported on nonlinear elastic foundations. *AIAA Journal*, **45**, 711–720 (2007)

[30] Li, S. R., Zhang, J. H., and Zhao, Y. G. Thermal post-buckling of functionally graded material Timoshenko beams. *Applied Mathematics and Mechanics* (*English Edition*), **27**(6), 803–810 (2006) DOI 10.1007/s10483-006-0611-y